Negative refractive index of metallic cross-I-shaped pairs: Origin and evolution with pair gap width

Y. G. Ma,* X. C. Wang, and C. K. Ong
Centre for Superconducting and Magnetic Materials, Department of Physics, National University of Singapore, Singapore 117542, Singapore

(Received 4 February 2008; published 29 July 2008)

A structured composite of the negative index of refraction was fabricated by one layer of cross-I-shaped metal pairs. In this structure, the electric and magnetic inclusions were effectively integrated into one small unit. We varied the spacing of the cross pair to control the location of the magnetic resonance mode and their intercoupling with the electric mode. The frequency dependences of permittivity, permeability, and refractive indices with different gap widths of the pairs were systematically discussed by free-space measurement as well as numerical simulation. A spacing window dependent on the geometrical parameters was found in which the real part of the refractive index could have a negative value. The one-layer cross-pair pattern proposed in this work can be extended to three-dimensional structures with well-controlled interlayer coupling that will greatly facilitate the fabrication and measurement of negative-index materials in high frequencies.

DOI: 10.1103/PhysRevE.78.016605 PACS number(s): 41.20.Jb, 78.20.Ci, 42.25.Fx

Negative-index materials (NIMs) have attracted great research interest in both scientific and engineering communities for their exotic and unique electromagnetic (EM) properties that are absent from conventional materials [1–3] and enable the construction of novel devices like superlens [4–7] or light trapper [8]. Negative-index behavior was initially predicted by Pendry in a composite consisting of metallic wire resonators for negative permittivity $\varepsilon(\omega)$ and splitting ring resonators for negative permeability $\mu(\omega)$ [9]. The negative EM scattering behavior was first experimentally demonstrated by Smith *et al.* in a microwave band using Pendry's topology [10]. Tremendous efforts have been made to optimize the structures of NIMs and push their spectrum range upward from microwave to THz [11]. Most of the previous structures were built on combinations of metallic wires and splitting rings. The fabrication process for such combinations would become rather difficult in higher frequencies in order to meet the requirements on the orientation and isolation of the electric and magnetic inclusions. In the optical region, arrays of splitting rings or their derivatives have been studied by several groups [12–15], but only regarding their magnetic responses. To improve the feasibility of NIMs in higher-frequency regions, the structure of the magnetic inclusion needs to be modified to realize a negative system in which the requirements on the orientations of the electric and magnetic components as well as the wave vector can be simultaneously fulfilled. Through theoretical simulations, Podolskiy *et al.* predicted pairs of metallic nanowires could have an optical negative refractive index behavior [16]. In their nanowire pairs, the electric mode was excited from the dipole resonance of the surface plasmons on the wires and the magnetic mode induced by the field coupling between the wire pairs. This architecture was implemented by Zhang *et al.* to fabricate a NIM in the near-infrared band [17]. The straight wire-pair structure was further modified by Zhou *et al.* into I-shaped wire pairs [18], in which the adjacent wires in one layer formed a *LC* resonance circuit which gave negative ε, while the wire pairs in neighboring layers formed a magnetic mode, leading to negative μ. Similar double-negative behavior in pairs of metallic crosses was recently predicted by another group with the additional advantages of improved polarization properties [19]. In these wire-pair structures, the requirements on the directions of the fields as well as the wave vector can be simultaneously satisfied. The multilayer design greatly simplifies the fabrication process for a three-dimensional NIM.

For the cross-pair pattern, since the electric and magnetic inclusions are effectively incorporated into one small unit, intermode coupling or disturbance will inevitably exist. The lattice constant or the spacing of the wire pairs should be deliberately controlled to form the double-negative resonance behaviors, about which, so far, there has been no discussion in previous publications. In this work, wire-pair structures were developed to fabricate a thin negative material in microwave bands using metallic cross-I-shaped patterns. The present cross-I configuration, other than the simple cross pattern as used in Ref. [19], had the advantage of easer tuning of the position of the electric mode. The spacing of the paired crosses was continuously modified to examine the influence of lattice constant on the resonance behaviors of the electric and magnetic modes and moreover their coupling or interdisturbance. The scattering spectrum was obtained by numerical calculation by Ansoft HFSS solution solver [20] as well as free-space measurement and the scatting parameters were used to retrieve the complex μ, ε, and n (refractive index) by well-known formulas [21]. We found that there was a small spacing window for the gap width between the cross-I pairs in which the double-negative resonance behaviors could be realized.

The metallic structures were experimentally fabricated by wet etching commercially available printed circuit boards (PCB FR4 used in this experiment with the substrate's $\varepsilon=4.4-i0.088$ and 35 μm copper clads coated) after lithography. The measured scattering spectra as well as the retrieved μ, ε, and n agreed well with the numerical predic-

*Corresponding author. phymy@nus.edu.sg

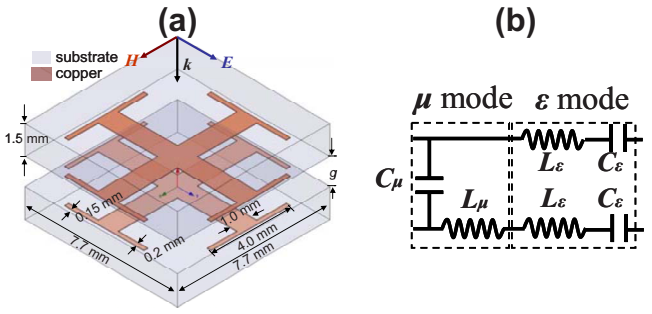

FIG. 1. (Color online) (a) Schematic structure and (b) equivalent circuit of the cross-pair pattern in one unit. The substrate material is FR4 with permittivity $\varepsilon=4.4-i0.088$ and coated by 35 μm copper clad. The orientations of the electric and magnetic components for the normal incident plane wave are also shown. The variable g denotes the spacing of the two cross pairs. In (b), L_μ and C_μ represent the wire-pair inductance and capacitance, and L_ε and C_ε represent the wire inductance and gap capacitance in the ε mode circuit on the substrate.

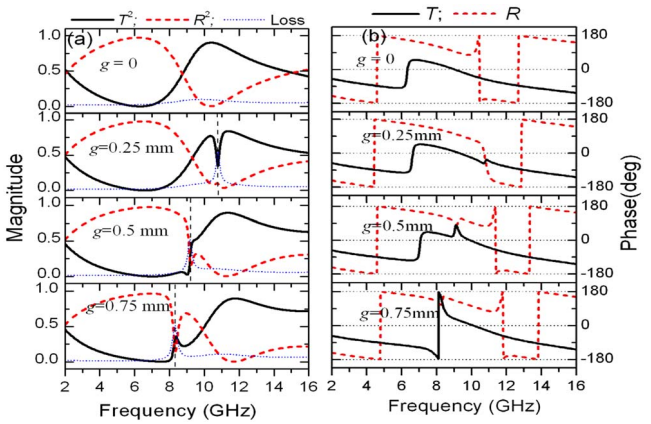

FIG. 2. (Color online) Simulated magnitude (a) and phase (b) spectra of the transmittance (black straight line) and reflectance (red dashed line) of the cross-pair patterns at different gap width g. The power loss $(=1-T^2-R^2)$ (blue dotted line) is also given in (a). Apart from the ε and μ modes, another resonance between 11 and 12 GHz, which was not mentioned in the text, can be identified from the reflectance curves (magnitude dip or sharp phase change) at different gap widths. Inspections of the current maps show that this mode is caused by a dipole resonance on the shorter and thinner wires located at the ends of the main wires of the cross.

tions. Figure 1(a) shows the schematic structures of our cross-pair pattern in one unit together with their size parameters, which is periodically infinite in the cross plane. It is formed by stacking two layers of cross-I arrays together with the patterns face to face. The variable g denotes the distance between the outer surfaces of the air-spaced crosses. The sample is normally illuminated by plane waves with the polarization direction parallel to one main axis of the copper cross. The magnetic component H is perpendicular to one of the wire pairs. In this design, the assembly of the conductive copper wires and the capacitive gaps at the I-shaped wire ends in one substrate are supposed to form the electric resonance circuit (ε mode), while the wire pairs between the two substrates form the magnetic circuit (μ mode). An equivalent circuit is given in Fig. 1(b) to approximate the EM response of the wire-pair structure. Here, L_μ and C_μ represent the wire pair's inductance and capacitance, while L_ε and C_ε represent the wire inductance and gap capacitance in the ε mode circuit on the substrate. Strictly, all these parameters are the functions of the gap width. It is seen that the electric and magnetic modes will be affected by each other due to their circuit connection.

Figures 2(a) and 2(b) show the simulated magnitude and phase spectra of the transmittance (black straight line) and reflectance (red dash line) from 2 to 16 GHz of the cross-pair patterns at different gap width g, respectively. The power loss $(=1-T^2-R^2)$ (blue dotted line) is also given in Fig. 2(a). First, at $g=0$ (corresponding to the case of single-layer crosses), the transmittance magnitude shows a wide dip around 6.3 GHz where the reflectance has a maximum. The corresponding transmittance phase in Fig. 2(b) increase sharply around 6.3 GHz, while the reflectance phase goes through a slow reduction untill 10 GHz (the upper part of the curve should be seen as connected to the lower portion by displacing −360°). The reflectance phase should be −180° at 6.3 GHz if the reference plane for reflection is deembedded to superimpose the upper surface of the cross. Around this frequency, numerical simulations show that the oscillation of the surface currents is greatly intensified on the arms with lengths parallel to the incident E field. Thus the ε mode should be excited with negligible resonance loss in this region.

When a 0.25-mm gap is introduced, as shown in Fig. 2(a), a narrow transmittance dip (reflectance peak) appears at 11.8 GHz where the loss reaches a maximum. This mode shifts to lower frequencies and towards the transmission dip as the gap width increases. Correspondingly, the transmittance dip induced by the newly excited mode at $g=0.25$ mm will gradually turn into a transmittance peak when g becomes larger. As shown in Fig. 2(b), both phase curves have sudden jerks at the frequency where this additional mode is excited. The magnitude of a jerk on the transmittance curve evolves to a −180° phase delay when $g\geqslant 0.75$ mm. When the gap is introduced, a circular conduction current is induced between the facing surfaces of the wire pairs, as typically shown in Figs. 3(a) and 3(b) for surface current maps of the cross pair of $g=0.5$ mm at 8.0 and 9.2 GHz, respectively. The intensity of the circular current will be greatly intensified when the new mode is excited, as shown in Fig. 3(b). Thus, this additional mode can be recognized as the μ mode arising from the LC resonance across the cross pairs. Furthermore, as shown in the bottom panel of Fig. 2(b), the transmittance phase for the pair of $g=0.75$ mm reduces monotonously as frequency increases (note that the phase curve should be displaced by −360° after 8.1 GHz). Reduction of the phase is accelerated around the μ-mode location. A similar phase spectrum of transmittance can be predicted in the cross-pair patterns of larger gaps. In simulations, the propagating wave has a phase factor of $\exp(-ink_0r)$, with k_0 the incident wave vector and r the propagation distance. The transmittance phase defined by $\Phi=-nk_0r$ should be a negative value for the wave propagating inside a material of positive index n. The phase relations

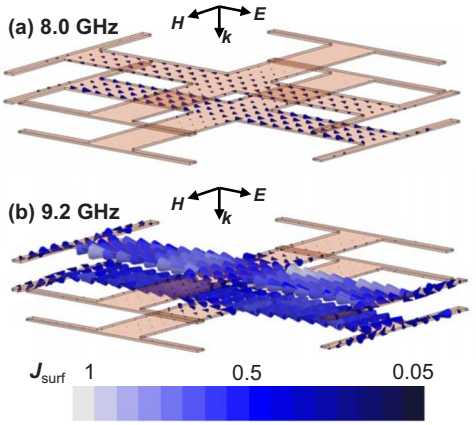

FIG. 3. (Color online) Snapshots of the surface currents on the metallic crosses with $g=0.5$ mm at (a) 8.0 and (b) 9.2 GHz together with the directions of the electric and magnetic fields of the incident wave at the same phase. The relative intensity of the current is described by the different colors and the sizes of the arrows. It is clear the currents in (a) shows an in-phase oscillation and out of phase in (b).

in the cross pairs of $g \geqslant 0.75$ mm reflect their positive wave refraction characters. Thus, one can see that for the wire-pair pattern the negative n can exist only within a limited range of gap width. In the present case the upper limit for g should be smaller than 0.75 mm.

We now consider the frequency location of the μ mode with respect to the gap width from the microwave transmission line theory. For a single parallel stripline pair filled by air, the scattering of microwaves at their ends can be regarded as an open condition (i.e., the capacitance of the end is zero) and its resonance frequency f is inversely proportional to the strip length l by $f=c_0/2\pi l$, where c_0 is the light velocity in vacuum. For the present structure, the resonance circuit for the μ mode is connected by finite gap capacitances ($C_{\varepsilon 1}$ and $C_{\varepsilon 2}$) at the wire ends, as shown in Fig. 1(b). The mode frequency can be estimated from the zero condition of the total impedance for the resonance circuit consisting of one portion of transmission line plus two parallel capacitances at the ends which can be written by

$$Z_g = -Z_w \frac{Z_g + iZ_w \cos(k_w l)}{Z_w + iZ_g \cos(k_w l)}, \tag{1}$$

with Z_w and Z_g being the effective impedances of the wire pair and the two ends, respectively, and k_w the propagation constant of the wire pair. Here $Z_w = \sqrt{\frac{\mu_0}{\varepsilon_0}\frac{g}{w}}$ (w is the wire width), $Z_g=(i2\pi f C_e)^{-1}$ (C_e is the total effective capacitance of the wire ends), and $k_w=2\pi f/c_0$. For the single-layer cross-I pattern, an analytical solution has been developed to evaluate C_e (the detailed formulas are given in Ref. [22]), which in this case is predicted to be nearly a constant around 0.28 pF in the frequency range of 2–16 GHz. By substituting all the parameters into Eq. (1), the obtained resonance frequencies at $g=0.25$ and 0.75 mm are 11.25 and 7.08 GHz, respectively. These values have reasonable agreement with the simulated results. The main discrepancy is due to the oversimplified approximations of C_e.

Figures 4(a)–4(c) show the spectra of permeability μ, permittivity ε, and refractive index n for the patterns of $g=0.25$, 0.5, and 0.75 mm, respectively, which are defined in the form of $m=m'-im''$. These quantities are retrieved by using the original Nicolson-Ross-Weir algorithm [21], which is mathematically identical to the formulas of Smith *et al.* without multiplying the transmittance by a phase factor [23]. At $g=0.25$ mm, ε shows a clear resonance behavior around 5.2 GHz, indicating excitation of the ε mode. The plasma frequency f_p (the upper frequency limit for $\varepsilon'<0$) is 10.1 GHz for the wire-pair structure. Thus the range for negative ε' is from 5.2 to 10.1 GHz. The real part of permeability μ' has an antiresonance character, and the imaginary part μ'' shows a negative peak associated with the electric resonance. Due to the finite spatial periodicity of the structures, the metallic composite arrays are normally of bounded refractive indexes [24]. As the bulk permittivity and permeability parameters have the relationship $n^2=\mu\varepsilon$, μ (ε) will show an antiresonance behavior if the ε (μ) mode is excited. Negative μ'' means an increased storage of magnetic energy inside the structure compensated for by the dissipated electric energy associated with the electric resonance. From the permeability curve in Fig. 4(a), a magnetic resonance can be identified near 11.8 GHz. The intensity of this mode is not

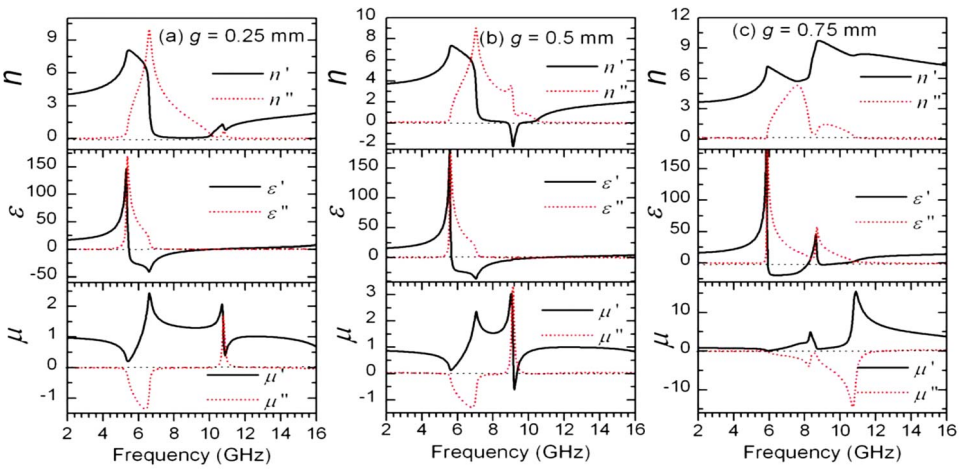

FIG. 4. (Color online) Numerically predicated spectra of permeability μ, permittivity ε, and refractive index n for the patterns of $g=$(a) 0.25, (b) 0.5, and (c) 0.75 mm, which are defined in the form of $m=m'-im''$ ($m=\mu$, ε, or n and $i=\sqrt{-1}$).

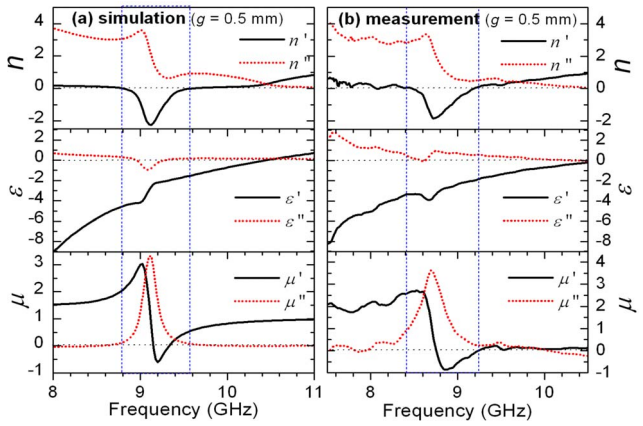

FIG. 5. (Color online) (a) Simulated and (b) measured parameters of μ, ε, and n of the cross-pair composite at $g=0.5$ mm in enlarged frequency regions. The dotted blue lines describe the frequency regions corresponding to negative n'.

strong enough to induce a negative μ' beyond the resonance frequency. Thus it corresponds to the positive refractive index n. When the gap width increases to 0.5 mm, as shown in Fig. 4(b), a small band corresponding to negative n' is successfully obtained around 9.2 GHz where μ' is negative resulting from the magnetic resonance. As shown in Figs. 3(a) and 3(b), the current loop formed at 8.0 GHz has an in-phase oscillation with the driving magnetic field, while it is out of phase at 9.2 GHz with larger intensity. When g further increases to 0.75 mm, the position of the magnetic mode is lowered to 8.2 GHz. No negative μ' or n' is induced in this case. The resultant ε spectra indicate that the original electric resonance is seemingly split into two isolated modes. It shows that the resonance behaviors for both electric and magnetic modes are seriously disturbed when they get too close in frequency due to the strengthened mode coupling. By refining the increment step of g, a gap window of $\sim$0.2 mm ($g=0.4-0.6$ mm) was found in which negative n' can be obtained.

Figures 5(a) and 5(b) show the simulated and measured parameters of μ, ε, and n of the cross pairs at $g=0.5$ mm in an enlarged scale of frequency regions, respectively. The sample was experimentally fabricated by stacking two layers of crosses (overall area 22×23 cm^2) together using pieces of paper strips as spacers. The scattering parameters $S11$ and $S21$ were measured by a pair of antennas connected to a vector network analyzer (HP 8722). The Nicolson-Ross-Weir algorithm was then applied to retrieve the constants of permittivity, permeability, and refractive index using the measured $S11$ and $S21$. It is seen that the experimentally obtained μ, ε, and n agree well with the simulated results. The small discrepancies in the frequency locations are mainly caused by the error in the thickness of the PCB spacing and the incidence of pseudo-plane-waves emitted from the antenna. It is noted that in this case excitation of the ε mode gives rise to a negative real permittivity with negligible imaginary part in a relatively very wide range from 7 to 10.6 GHz. So the band for the double-negative resonance behavior will be mainly determined by the frequency of the μ mode. As indicated by the blue dotted lines in the figures, the bandwidth for negative n' has a closer correlation with the peak width of μ'', rather than the width of negative μ'. It is mathematically understandable since μ'' should have an equal contribution to n as μ' in terms of the formula $n=[(\mu'-i\mu'')(\varepsilon'-i\varepsilon'')]^{1/2}$ [17]. The simulations predict that raising the loss constant ($\tan\delta$) of the PCB substrate will broaden the peak width of μ'', which in turn widens the bandwidth of negative n'. Such a loss dependence is the typical character for a Lorentz-type resonance resulting from the strengthened damping effect. In this case, it leads to a band of negative real index around 9 GHz with a bandwidth of 0.8 GHz. For our cross-I pairs, which are of the character of biaxial anisotropies, this negative window is expected to have a low dependence on the polarization angle φ of the incident wave. This point has been experimentally verified by the independence relationships of transmittance and reflectance versus φ (not shown here). But the spatially distribution feature for the basic unit will make the resonance modes inevitably dispersive. The simulations show that the negative-index window will displace towards higher frequency by 0.3 GHz when the incident angle θ is increased to 20° for both TE and TM mode. Since the peak width at the half maximum for negative n' is also $\sim$0.3 GHz, the dispersive degree for refraction may be acceptable at $\theta<20°$. This upper limit is believed to be further increased by optimizing the wire structures and permittivity of the dielectric filler.

It should be mentioned that excitation of the μ mode will concentrate strong EM energy inside the structure, which is also the reason for the increased loss at the μ-mode locations. This energy concentration effect can greatly enhance the transmission efficiency of the metallic cross pairs irrespective of the sign of the refractive index. It behaves like Fabry-Perot mode-induced wave transmission over subwavelength slits in metallic gratings [25]. Thus the transmission bands at $g\geqslant0.75$ mm can be induced only regarding to the magnetic resonance. On the other hand, it should be noted that the interaction of the paired crosses can have a great influence on the wave scattering only around the frequency region where the μ mode is excited. This point can be understood from the comparison of the scattering coefficients of the cross pairs at different g, as shown in Figs. 2(a) and 2(b). Outside this region, the cross pairs can be simply regarded as two isolated impedance layers sandwiching an air gap. Thus, it is totally possible to build a three-dimensional NIM by repeating the cross-pair assembly in the wave propagation direction in which the near-field coupling between adjacent assemblies is effectively reduced by a suitable spacing.

In summary, the influences of the gap width on the wave scattering and the refractive index of cross-I pairs have been studied. The circuit connection of the electric and magnetic constitutes in this structure makes their resonance behaviors highly sensitive to the gap width. The magnetic mode should be deliberately controlled by adjusting the gap width to avoid the situation of too weak resonations where there is a small gap or strong couplings with the electric mode where there is a large gap. By repeating the cross-pair bilayer structure along the wave-vector direction, a three-dimensional negative-index material can be highly anticipated.

We thank Dr. X. S. Rao for discussions at the early stage of the work and A^*STAR for funding.

[1] R. A. Shelby, D. R. Smith, and S. Schultz, Science **292**, 77 (2001).
[2] G. V. Eleftheiades and K. G. Balmain, *Negative Refraction Metamaterials: Fundamental Principles and Applications* (Wiley-IEEE, Hoboken, NJ, 2005).
[3] C. G. Parazzoli, R. B. Greegor, K. Li, B. E. C. Koltenbah, and M. Tanielian, Phys. Rev. Lett. **90**, 107401 (2003).
[4] J. B. Pendry, Phys. Rev. Lett. **85**, 3966 (2000).
[5] X. S. Rao and C. K. Ong, Phys. Rev. B **68**, 113103 (2003).
[6] T. Taubner, D. Korobkin, Y. Urzhumov, G. Shvets, and R. Hillenbrand, Science **313**, 1595 (2006).
[7] H. Lee, Z. Liu, Y. Xiong, C. Sun, and X. Zhang, Opt. Express **15**, 15886 (2007); Z. Liu, H. Lee, Y. Xiong, C. Sun, and X. Zhang, Science **315**, 1686 (2007).
[8] K. L. Tsakmakidis, A. D. Boardman, and O. Hess, Nature (London) **450**, 397 (2007).
[9] J. B. Pendry, A. J. Holden, D. J. Robbins, and W. J. Stewart, IEEE Trans. Microwave Theory Tech. **47**, 2075 (1999).
[10] D. R. Smith, W. J. Padilla, D. C. Vier, S. C. Nemat-Nasser, and S. Schultz, Phys. Rev. Lett. **84**, 4184 (2000); R. A. Shelby, D. R. Smith, and S. Schultz, Science **292**, 77 (2001).
[11] See the review articles and the references therein in S. A. Ramakrishna, Rep. Prog. Phys. **68**, 449 (2005); C. M. Soukoulis, M. Kafesaki, and E. N. Economou, Adv. Mater. (Weinheim, Ger.) **18**, 1941 (2006); W. J. Padilla, D. N. Basov, and D. R. Smith, Mater. Today **9**, 28 (2006).
[12] N. Wongkasem, A. Akyurtlu, J. Li, A. Tibolt, Z. Kang, and W. D. Goodhue, PIER **64**, 205 (2006).
[13] T. J. Yen, W. J. Padilla, N. Fang, D. C. Vier, D. R. Smith, J. B. Pendry, D. N. Basov, and X. Zhang, Science **303**, 1494 (2004).
[14] S. Linden, C. Enkirch, M. Wegener, J. Zhou, T. Koschny, and C. M. Soukoulis, Science **306**, 1351 (2004).
[15] S. Zhang, W. J. Fan, B. K. Minhas, A. Frauenglass, K. J. Malloy, and S. R. J. Brueck, Phys. Rev. Lett. **94**, 037402 (2005).
[16] V. A. Podolskiy, A. K. Sarychev, and V. M. Shalaev, Opt. Express **11**, 735 (2003).
[17] S. Zhang, W. Fan, N. C. Panoiu, K. J. Malloy, R. M. Osgood, and S. R. J. Brueck, Phys. Rev. Lett. **95**, 137404 (2005).
[18] J. F. Zhou, T. Koschny, L. Zhang, G. Tuttle, and C. M. Soukoulis, Appl. Phys. Lett. **88**, 221103 (2006).
[19] C. Imhof and R. Zengerle, Opt. Express **14**, 8257 (2006).
[20] Ansoft HFSS is a full wave electromagnetic solution solver based on a finite-element method. It treats the metal scattering by using the surface-impedance boundary condition at the dielectric/metal interface. The latest version of Ansoft HFSS 11 allows using the Floquet-Port excitation to simulate the model of free-space plane-wave illumination on an infinite sample. In our simulation, the scattering parameters $S11$ and $S21$ are obtained with reference planes superimposed with the top and bottom surfaces of the unit cell shown in Fig. 1(a). Our convergence condition is that the differences of $S11$ and $S21$ <0.005 for two successive adaptive passes.
[21] A. M. Nicolson and G. F. Ross, IEEE Trans. Instrum. Meas. **19**, 377 (1970); W. B. Weir, Proc. IEEE **62**, 33 (1974).
[22] C. R. Simovski, P. de Maagt, and I. V. Melchakova, IEEE Trans. Antennas Propag. **53**, 908 (2005).
[23] D. R. Smith, S. Schultz, P. Markos, and C. M. Soukoulis, Phys. Rev. B **65**, 195104 (2002).
[24] T. Koschny, P. Markos, D. R. Smith, and C. M. Soukoulis, Phys. Rev. E **68**, 065602(R) (2003).
[25] Y. G. Ma, X. S. Rao, G. F. Zhang, and C. K. Ong, Phys. Rev. B **76**, 085413 (2007).